Axl and Growth Arrest–Specific Gene 6 Are Frequently Overexpressed in Human Gliomas and Predict Poor Prognosis in Patients with Glioblastoma Multiforme

Markus Hutterer,[1,5] Pjotr Knyazev,[5] Ariane Abate,[1] Markus Reschke,[5] Hans Maier,[2] Nadia Stefanova,[1] Tatjana Knyazeva,[5] Verena Barbieri,[4] Markus Reindl,[1] Armin Muigg,[1] Herwig Kostron,[3] Guenther Stockhammer,[1] and Axel Ullrich[5,6]

Abstract

Purpose: The receptor tyrosine kinase Axl has recently been identified as a critical element in the invasive properties of glioma cell lines. However, the effect of Axl and its ligand growth arrest–specific gene 6 (Gas6) in human gliomas is still unknown.

Experimental Design: Axl and Gas6 expression was studied in 42 fresh-frozen and 79 paraffin-embedded glioma specimens by means of reverse transcription-PCR and immunohistochemistry. The prognostic value of Axl and Gas6 expression was evaluated using a population-based tissue microarray derived from a cohort of 55 glioblastoma multiforme (GBM) patients.

Results: Axl and Gas6 were detectable in gliomas of malignancy grades WHO 2 to 4. Moderate to high Axl mRNA expression was found in 61%, Axl protein in 55%, Gas6 mRNA in 81%, and Gas6 protein in 74% of GBM samples, respectively. GBM patients with high Axl expression and Axl/Gas6 coexpression showed a significantly shorter time to tumor progression and an association with poorer overall survival. Comparative immunohistochemical studies showed that Axl staining was most pronounced in glioma cells of pseudopalisades and reactive astrocytes. Additionally, Axl/Gas6 coexpression was observed in glioma cells and tumor vessels. In contrast, Axl staining was not detectable in nonneoplastic brain tissue and Gas6 was strongly expressed in neurons.

Conclusions: In human gliomas, Axl and Gas6 are frequently overexpressed in both glioma and vascular cells and predict poor prognosis in GBM patients. Our results indicate that specific targeting of the Axl/Gas6 signaling pathway may represent a potential new approach for glioma treatment.

Glioblastoma multiforme (GBM) is the most common and most aggressive primary brain tumor in adults with an incidence of 5 to 8 per 100,000 inhabitants per year (1, 2). Advances in surgery, radiotherapy, and chemotherapy do only have a minor effect on the natural course of this tumor with a mean overall survival (OS) time of only 9 to 15 months from the time of diagnosis (2, 3). Therefore, there is an urgent need for more effective therapeutic approaches based on a better understanding of the molecular mechanisms of GBM growth, invasiveness, and vascularization.

The receptor tyrosine kinase Axl is characterized by an extracellular domain consisting of two immunoglobulin-like domains in juxtaposition to two fibronectin type III domains (4, 5), typical for cell adhesion molecules of the immunoglobulin superfamily (6). The growth arrest–specific gene 6 (Gas6) is the natural ligand of Axl (7, 8). Axl/Gas6 signaling has been shown to regulate survival, proliferation, and migration in a variety of cells *in vitro*, including tumor-derived cell lines of epithelial, mesenchymal, and hematopoietic origin (5, 9). Recently, Axl has been identified to be overexpressed in the majority of glioma cell lines and was associated with invasive properties of glioma cell lines in a spheroid as well as in a xenograft mouse model (10). However, the biological effect of Axl and its ligand Gas6 in human gliomas is still unknown.

In this study, we investigated the mRNA and protein expression of Axl and Gas6 in human gliomas WHO grades 2 to 4, determined its staining pattern in comparison with nonneoplastic brain tissue derived from epilepsy surgery, and compared the Axl and Gas6 protein expression with the clinical course of patients with GBM.

Authors' Affiliations: [1]Clinical Department of Neurology, [2]Institute of Pathology, [3]Clinical Department of Neurosurgery, and [4]Department of Medical Statistics, Informatics and Health Economics, Innsbruck Medical University, Innsbruck, Austria; [5]Department of Molecular Biology, Max Planck Institute of Biochemistry, Munich/Martinsried, Germany; and [6]Center of Molecular Medicine, Institute of Molecular and Cell Biology, Singapore, Singapore

Received 4/11/07; revised 9/5/07; accepted 10/8/07.

Grant support: Medizinischer Forschungsfond Tirol grant 120/2005 (G. Stockhammer) and Austrian Cancer Society, Krebshilfe Tirol grant 23/2005 (G. Stockhammer).

The costs of publication of this article were defrayed in part by the payment of page charges. This article must therefore be hereby marked *advertisement* in accordance with 18 U.S.C. Section 1734 solely to indicate this fact.

Note: M. Hutterer and P. Knyazev contributed equally as first authors. A. Ullrich and G. Stockhammer contributed equally as senior authors.

The authors confirm the originality of this study and disclose previous reports or publications. In part, preliminary results of this study were presented at the 7th Congress of the European Association for Neurooncology, September 14-17, 2006, Vienna, Austria (poster presentation).

Requests for reprints: Markus Hutterer, Clinical Department of Neurology, Innsbruck Medical University, Anichstrasse 35, A-6020 Innsbruck, Austria. Phone: 43-512-504-24365; Fax: 43-512-504-24266; E-mail: Markus.Hutterer@i-med.ac.at.

doi:10.1158/1078-0432.CCR-07-0862

Materials and Methods

Fresh-frozen tissue. This study was done according to the ethical regulative of the institutional review board. During open neurosurgery, tissue samples from brain tumor patients were snap frozen in liquid nitrogen within 3 min of harvesting and stored at -80°C. mRNA expression levels of Axl, Gas6, and *tubulin* (housekeeping gene) were investigated using reverse transcription-PCR.

Total RNA isolation and cDNA synthesis. Total RNA was isolated from 42 fresh-frozen glioma specimens using the acid guanidium thiocyanate-phenol-chloroform extraction method (11). After NaCl acetate treatment to reduce genomic DNA, total RNA was extracted with phenol-chloroform, precipitated with isopropanol, resuspended with lysis buffer, reprecipitated with isopropanol, washed with 80% ethanol, and finally solved in TES/diethyl pyrocarbonate solution. Afterwards, the total RNA concentration was determined by absorbance measurement (260 and 280 nm) and the quality of total RNA was verified by a 1% agarose gel electrophoresis. Only samples with 28S/18S ratios >2 and with no evidence of DNA contamination and RNA degradation were used for continuative cDNA synthesis. cDNA synthesis was done using 5 μg of total RNA in an oligo(dT) primer mix (1 pmol, total volume 9 μL; Chipco), which was heated at 70°C for 3 min and then cooled on ice. A mastermix containing 5× reverse transcriptase buffer, 10 mmol/L deoxynucleotide triphosphates, 100 mmol/L DTT, 1 unit (0.5 μL) RNase inhibitor, and 50 units (2 μL) avian myeloblastosis virus reverse transcriptase (Molecular Diagnostics, Roche) for each cell line and frozen tumor sample was added into a tube and subsequently heated at 42°C for 2 h. A stop reaction was done with 80 μL Tris-EDTA 10/0.1 followed by heating at 72°C for 7 min. The quality of the cDNA was verified using a 1.5% agarose gel electrophoresis. Afterwards, the cDNA probe was denatured with 10 μL 1 N NaOH, pH neutralized with 5 μL 2 N HCl and 5 μL 2 mol/L Tris-HCl (pH 7.5), and purified using the QIAquick PCR Purification kit (Qiagen) according to the manufacturer's instructions.

PCR. The PCR method was used to determine mRNA expression levels of Axl, Gas6, and *tubulin* (housekeeping gene) in fresh-frozen glioma samples. The following primer sequences were applied: Axl, 5′-GGTGGCTGTGAAGACGATGA-3′ (forward) and 5′-CTCAGATACTC-CATGCCACT-3′ (reverse); Gas6, 5′-ACATCTTGCCGTGCGTGCCCTTCA-3′ (forward) and 5′-ATTCCGCGCCAGCTCCTCAACAGA-3′ (reverse); and *tubulin*, 5′-AAGTGACAAGACCATTGGGGGAGG-3′ (forward) and 5′-GGGCATAGTTATTGGCAGCATC-3′ (reverse). All primers were synthesized by MWG Biotech. PCR was done using 1 μL cDNA as template in a mastermix containing 10× PCR buffer without $MgCl_2$, 25 mmol/L $MgCl_2$, 10 mmol/L deoxynucleotide triphosphates, 10 pmol/μL of each specific primer, and 0.5 IU Taq DNA polymerase (Fermentas Taq Polymerase kit, Roche) for each sample and carried out in a DNA thermal cycler (Eppendorf). PCR cycling conditions began with an initial DNA denaturation step at 94°C for 2 min followed by 32 cycles at 94°C for 30 s, 55°C for 30 s, and 72°C for 30 s. Amplified PCR products were applied to a 2% agarose gel for electrophoresis done at 80 V for 30 min. To analyze the mRNA expression frequency, reverse transcription-PCR results were evaluated semiquantitatively (no, low, moderate, or high).

Whole tissue sections and tissue microarray population. To investigate the immunohistochemical staining patterns of Axl and Gas6 protein in neoplastic and nonneoplastic tissue samples, we applied representative whole sections of paraffin-embedded glioma tissue WHO grades 2 to 4 (30 samples) and nonneoplastic hippocampal tissue derived from epilepsy surgery (10 samples). For clinicopathologic correlation studies,

Table 1. Clinical characteristics of 76 patients with gliomas included in the population-based TMA

Variable	Histologic classification (WHO)		
	Grade 4	Grade 3	Grade 2
No. patients	55	6	15
Age,* y (range)	56.5 (18-78)	56.4 (47-69)	41.8 (26-60)
≥60	24	1	2
<60	31	5	13
Sex			
Female	20	1	6
Male	35	5	9
KPS,† mean (range)	81.5 (70-100)	85.0 (80-90)	88.7 (80-100)
≥80	42	6	15
<80	13	0	0
Tumor location			
Frontal	20	1	9
Nonfrontal	35	5	6
Extend of resection‡			
Total and subtotal	26§	4	8
Partial	26§	2	7
Chemotherapy			
+	40	5	0
-	15	1	15
Radiation‖			
+	45	5	8
-	10	1	7
TTP, mo (range)	7.3 (1.6-17.0)	9.5 (9.4-9.6)	44.1 (6.0-64.0)
OS, mo (range)	12.6 (0.8-27.5)	30.2 (10.8-59.5)	72.0 (30.0-102.5)

*Age at first diagnosis.
†Only patients KPS ≥ 70 were included.
‡In first-line treatment, all GBM patients had undergone open surgery with either macroscopically total/subtotal or partial tumor resection.
§Incomplete clinical data.
‖No radiation: five primary and five secondary GBM.

Table 2. Axl and Gas6 mRNA and protein expression frequency in human gliomas WHO grades 2 to 4

	mRNA expression (RT-PCR)*				Protein expression (IHC) †			
	n ‡	Axl§	Gas6§	Axl/Gas6§	*n* ‡	Axl§	Gas6§	Axl/Gas6§
Grade 4	31	19 (61)‖	25 (81)‖	19 (61)‖	55	30 (55)‖	41 (75)‖	22 (43)‖
GBM primary	24	13 (54)	19 (79)	13 (54)	46	24 (52)	33 (72)	18 (42)
GBM secondary	7	6 (85)	6 (85)	6 (86)	9	6 (66)	8 (89)	4 (44)
Grade 3	6	5 (83)‖	6 (100)‖	5 (83)‖	6	4 (67)‖	4 (67)‖	4 (67)‖
Astrocytoma	3	3 (100)	3 (100)	3 (100)	4	2 (50)	2 (50)	2 (50)
Oligodendroglioma	2	1 (50)	2 (100)	1 (50)	1	1 (100)	1 (100)	1 (100)
Oligoastrocytoma	1	1 (100)	1 (100)	1 (1)	1	1 (100)	1 (100)	1 (100)
Grade 2	1	—	—	—	15	11 (73)‖	10 (67)‖	6 (40)‖
Astrocytoma	1	—	—	—	7	6 (86)	5 (71)	3 (43)
Oligodendroglioma	—	—	—	—	2	1 (50)	1 (50)	1 (50)
Oligoastrocytoma	—	—	—	—	6	4 (66)	4 (67)	2 (33)

Abbreviations: RT-PCR, reverse transcription-PCR; IHC, immunohistochemistry.
*mRNA expression frequency was quantified semiquantitatively (no, low, moderate, or high).
† Protein expression frequency was analyzed using the GIS by dividing into low/no (GIS 0-4), moderate (GIS 5-8), and high (GIS 9-12) values.
‡ Number of cases.
§Number of cases with moderate to high expression levels (percentage).
‖No significant differences in expression frequencies between gliomas grading 2, 3, and 4 (Kruskal-Wallis test).

a population-based tissue microarray (TMA) was constructed containing paraffin-embedded tumor samples from 24 adult patients with newly diagnosed glioma WHO grades 2 to 3 and 55 patients with newly diagnosed GBM WHO grade 4 (Tables 1 and 2).

TMA construction. Tissue from brain tumor patients (1996-2005) treated by open surgery with partial, subtotal, or total tumor resection was routinely fixed in 4% formaldehyde solution and embedded in paraffin. For TMA construction, paraffin blocks were retrieved from the files of the Institute of Pathology, Innsbruck Medical University. The histologic diagnosis of the gliomas follows the WHO classification and grading system (1). The neuropathologic findings were confirmed by a board-certified neuropathologist, and representative tumor areas for TMA cores were identified on H&E-stained slides. Using a tissue microarrayer (MTA-1, Beecher Instruments), the paraffin blocks were punched with a diameter of 0.6 mm and the core was transferred to a recipient block. From each brain tumor, triplicate cores of different sites of the most representative tumor regions were collected. Finally, five recipient blocks were heated at 60°C for 30 min and subsequently cooled for 24 h. TMA blocks were cut into 4-μm sections and placed onto coated slides (PSA-4x, Instrumedics, Inc.) using an adhesive tape transfer system (Paraffin Tape Transfer System, Instrumedics).

Immunohistochemistry. Whole sections of formalin-fixed, paraffin-embedded glioma specimen derived from tumor surgery and nonneoplastic hippocampal brain samples derived from epilepsy surgery were studied for Axl and Gas6 staining patterns. The sections were deparaffinized in xylene (2 × 20 min) and rehydrated through a descending concentration sequence of ethanol. Heat-induced epitope retrieval was done by boiling the slides in NaCl citrate buffer (pH 6.0) using a microwave (2 × 8 min, 750 W). Afterwards, the slides were cooled for 30 min at room temperature within the buffer. Nonspecific staining was blocked by 5% H_2O_2 in 0.3% PBS-Triton X-100 (15 min) and 10% normal horse serum in 0.3% PBS-Triton X-100 (60 min). Incubation with primary Axl and Gas6 antibodies (1:100 dilution in 1% normal horse serum/0.3% PBS-Triton X-100) was carried out overnight at 4°C. Antibodies were purchased from the following suppliers: mouse monoclonal anti-human Axl (MAB 423-36; Max Planck Institute of Biochemistry, Department of Molecular Biology, Martinsried/Munich, Germany; antibody specificity was proved by Western blot and fluorescence-activated cell sorting) and goat polyclonal anti-human Gas6 (C-20, Santa Cruz Biotechnology). The bound primary antibody was detected by a biotinylated anti-mouse (Axl) or biotinylated anti-goat (Gas6) IgG secondary antibody (both made in horse; 60 min; Vector Laboratories, Inc.). The staining sensitivity was increased using the Vectastain Elite ABC Kit PK-6100 Standard as described in the supplier's manual, and the reaction was visualized through incubation with liquid substrate 3,3′-diaminobenzidine tetrahydrochloride (Sigma) for 5 min. Afterwards, the slides were counterstained with Meyer's hemalaun (Merck), mounted with Entellan (Merck), and coverslipped. Negative controls were included in each batch replacing the primary or secondary antibody and staining with an isotype-matched IgG2 monoclonal antibody.

Immunohistochemical staining of glial fibrillary acidic protein (GFAP), neurofilament proteins, and Ki-67 was done according to the manufacturer's standard protocols in a pathologic routine laboratory (Institute of Pathology, Medical University of Innsbruck). Antibodies were purchased from the following suppliers: rabbit polyclonal anti-human GFAP (Dako), mouse monoclonal anti-human Ki-67 (MIB-1, Dako), and mouse monoclonal anti-human neurofilament proteins (Biogenex). Immunohistochemical pictures were taken using a Nikon Eclipse E800 microscope.

Neuropathologic evaluation. Staining pattern and intensity were evaluated by a board-certified neuropathologist. At least two of three TMA spots had to be representative. A semiquantitative scoring system was applied following the German immunohistochemical score (GIS; ref. 12). Percentage of positive cells was graded as 0 (negative), 1 (up to 10%), 2 (11-50%), 3 (51-80%), or 4 (>80% positive cells) and staining intensity as 0 (no staining), 1 (weak), 2 (moderate), or 3 (strong). The final immunoreactive GIS was defined as the multiplication of both grading results (percentage of positive cells × staining intensity). Protein expression frequencies were analyzed by dividing the GIS into no/low (GIS < 5), moderate (GIS ≥ 5 to GIS ≤ 8), and high (GIS > 8) levels. For evaluation of the prognostic effect of Axl and Gas6, high or low protein expression levels were considered through GIS dichotomization at the median (GIS ≤ 6 versus GIS > 6). Axl/Gas6 coexpression was determined by a GIS >6 of both Axl and Gas6.

Statistical analysis. Statistical analysis was done using the variables time to tumor progression (TTP), progression-free survival at 6 months (PFS6), OS, and OS at 12 months (OS12). TTP and OS were determined in months from the date of surgery of a primary or secondary GBM. TTP end points corresponded with the detection of a recurrent tumor by magnetic resonance imaging or computed tomography. Survival end points matched to dates of death or follow-up end points. Patients who were alive at the follow-up date were censored for survival analyses. Kaplan-Meier curves were plotted to

estimate TTP and OS as a function of Axl and/or Gas6 expression and group differences were assessed by the log-rank method. Adjusted analysis of the effect of Axl and Gas6 protein expression on TTP and OS in glioblastoma patients was carried out by multivariate data analysis using the Cox proportional hazards regression model. The following clinically relevant variables were considered for statistical analysis: age (<60 versus ≥60 years), Karnofsky performance scale (KPS; <80 versus ≥80), tumor location (frontal versus nonfrontal), extend of resection (partial versus total/subtotal resection), chemotherapy (+ versus -), and radiation (+ versus -). The forward stepwise procedure using 95% confidence intervals was adopted to determine the independent prognostic value of Axl and Axl/Gas6 expression in multivariate analysis (Table 3; patients with a KPS <70 and patients with stereotactic or open biopsy were not included in this study). Multivariable binary logistic regression analysis, including age, KPS, tumor location, extend of resection, chemotherapy, and radiation as covariables, was done to evaluate the association of Axl and Gas6 expression with PFS6 and OS12. Differences of expression frequencies between glioma subgroups (WHO grades 2/3/4) and primary and secondary GBM were evaluated by the Kruskal-Wallis test. Statistical analysis was done using Statistical Package for the Social Sciences 12.0 software (SPSS, Inc.) and *P* values of <0.05 were considered statistically significant.

Results

Axl and Gas6 are frequently overexpressed in human gliomas. Reverse transcription-PCR studies of fresh-frozen tumor samples (Fig. 1A) and immunohistochemical studies of paraffin-embedded tumor tissue (Fig. 1B-G) showed that Axl and Gas6 are frequently overexpressed in gliomas WHO grades 2 to 4, including astrocytic, oligodendroglial, and ependymal origin (Table 2). In GBM WHO grade 4, moderate to high expression levels were found for Axl mRNA in 61% (n = 19), for Axl protein in 55% (n = 30), for Gas6 mRNA in 81% (n = 25), and for Gas6 protein in 75% (n = 41), respectively. Axl/Gas6 coexpression was detectable in 61% (n = 19) at the mRNA and in 43% (n = 22) at the protein level. The Kruskal-Wallis test showed no significant differences of Axl and/or Gas6 expression frequencies between the glioma subgroups WHO grades 2/3/4 as well as primary and secondary GBM (Table 2). In contrast to tumor tissue (Fig. 2A), Axl protein was not detectable in nonneoplastic brain tissue distant to the tumor (Fig. 2B) or hippocampal brain tissue derived from epilepsy surgery (data not shown). However, Gas6 showed a pronounced neuronal membrane and cytoplasmatic granular staining in nonneoplastic brain tissue (data not shown).

Axl and Gas6 expression shows a distinct cellular distribution pattern in GBM. A characteristic immunohistochemical finding was a membrane-accentuated Axl staining of glioma cells (Fig. 2A-D), particularly of pseudopalisades (Fig. 2C and D) and opposing tumor cells (Fig. 2D). In addition, vessels within a necrotic area were typically surrounded by Axl- and GFAP-positive tumor cells (Fig. 2E), representing necrotic areas and pseudopalisades caused by intravascular thrombosis. In corresponding tissue sections, pseudopalisades showed a weak Gas6 expression (Fig. 2F) and staining of the proliferation marker Ki-67 revealed less proliferative potential of glioma cells within pseudopalisades and necrotic areas compared with adjacent tumor cells (Fig. 2F). In nonpseudopalisading GBM cells, Axl and Gas6 were frequently found to be coexpressed (Fig. 1F and G).

A second distinct neuropathologic finding was that both Axl (Fig. 2G and H) and Gas6 (data not shown) were strongly expressed in endothelial cells of microvascular hyperplasia and tumor cells adjacent to microvascular hyperplasia showed a pronounced Axl staining (Fig. 2G). Furthermore, arterioles and venules in the peripheral infiltrating zone were characterized by Axl (Fig. 2I) and Gas6 (data not shown) expression of endothelial cells, vascular smooth muscle cells, and pericytes. In contrast, vessels of nonneoplastic brain tissue showed neither Axl nor Gas6 staining (data not shown).

A third characteristic feature was a prominent Axl staining of reactive astroglial cells, which were identified by their astrocytic morphology, positive GFAP expression, and negative neurofilament protein staining (Fig. 2J-L). Such reactive astrocytes were observed in the peripheral GBM infiltrating zone enchased by tumor cells (Fig. 2J and K). Typically, reactive astroglial cells showed Axl/GFAP coexpression, a pronounced Axl staining of

Table 3. Multivariate survival analysis (forward LR method) of Axl and Gas6 protein expression in GBM patients

Variable	TTP		OS
	HR (95% CI)	*P*	*P*
Axl GIS (≤6 vs >6)	3.2 (1.5-6.8)	0.001	0.09
Age (≥60 vs <60)		NS	NS
KPS (≥80 vs <80)		NS	NS
Tumor location (frontal vs nonfrontal)		NS	NS
Extend of resection (total/subtotal vs partial)		NS	NS
Chemotherapy (+ vs -)		NS	NS
Radiation (+ vs -)		NS	NS
Axl/Gas6 GIS (≤6 vs >6)	3.6 (1.5-8.4)	0.003	0.142
Age (≥60 vs <60)		NS	NS
KPS (≥80 vs <80)		NS	NS
Location (frontal vs nonfrontal)		NS	NS
Resection (total/subtotal vs partial)		NS	NS
Chemotherapy (+ vs -)		NS	NS
Radiation (+ vs -)		NS	NS

NOTE: Gas6 expression alone was not significant (TTP: P = 0.392; OS: P = 0.144).
Abbreviations: NS, not significant; HR, hazard ratio; 95% CI, 95% confidence interval.

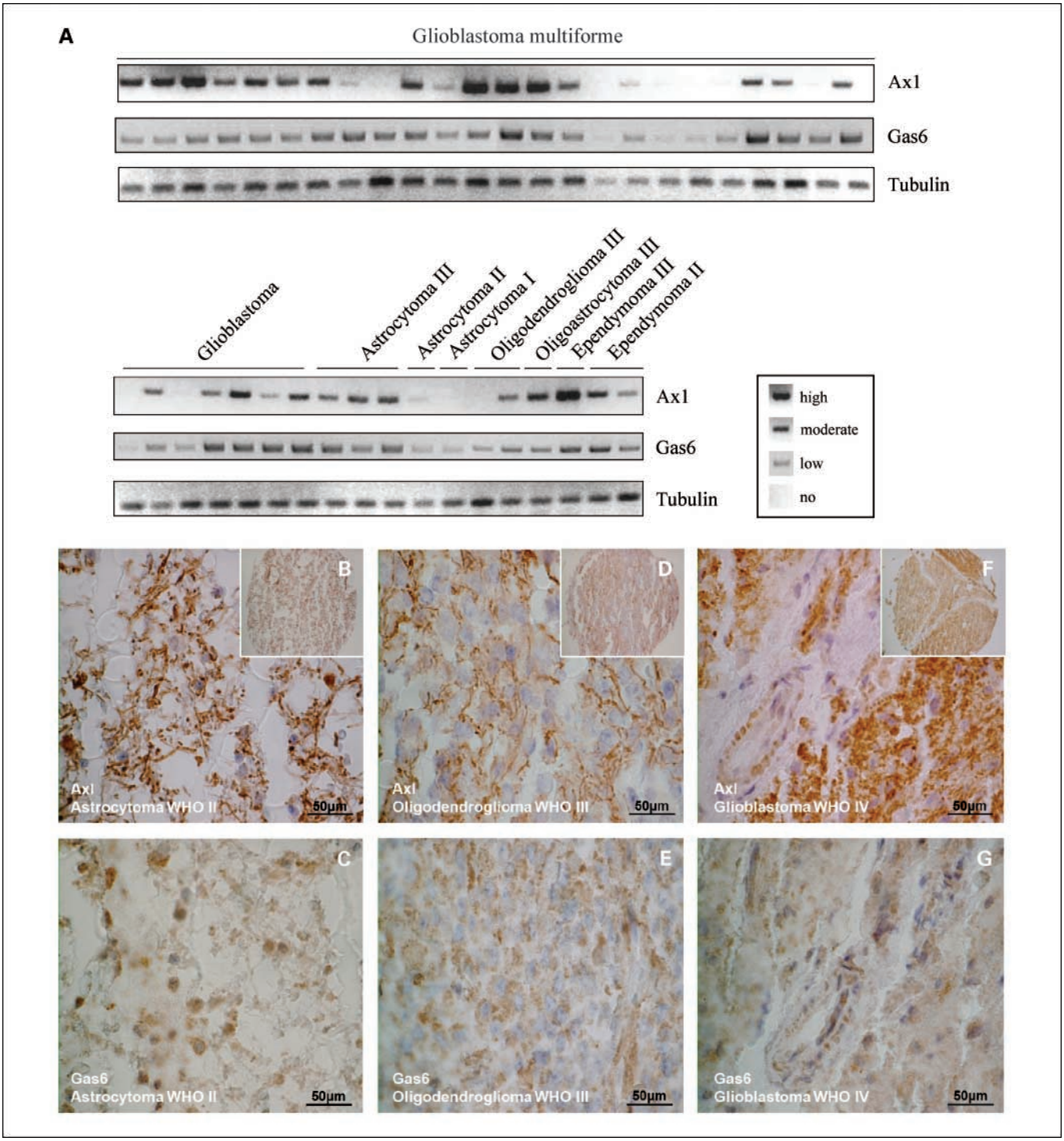

Fig. 1. Reverse transcription-PCR and immunohistochemical staining of Axl and Gas6 in human gliomas. *A,* mRNA expression of Axl, Gas6, and *tubulin* in human fresh-frozen glioma samples. mRNA expression frequency was evaluated semiquantitatively (no, low, moderate, or high). *B* to *G,* immunohistochemical staining pattern of Axl and Gas6 in gliomas WHO grades 2 to 3 of astrocytic and oligodendroglial origin and GBM WHO grade 4 (TMA spots).

the astrocytic end feet, and a weak Gas6 staining (Fig. 2L). However, Axl, Gas6, and GFAP expression was absent in vessels and astrocytes more distant to the GBM (data not shown).

Axl and Gas6 expression correlates with poor prognosis in GBM patients. Using a population-based TMA, we assessed the prognostic value of Axl and Gas6 expression in GBM patients. Evaluation of Axl expression revealed a median TTP of 8.9 months (range, 6.1-17.0) for patients with low (n = 19, GIS $\leq$ 6) and 3.9 months (range, 1.6-10.0) for patients with high Axl expression values (n = 16, GIS > 6; P < 0.001 by the log-rank test, Fig. 3A). The adjusted hazard ratio for TTP was 3.2 (95% confidence interval, 1.5-6.8) in patients with high

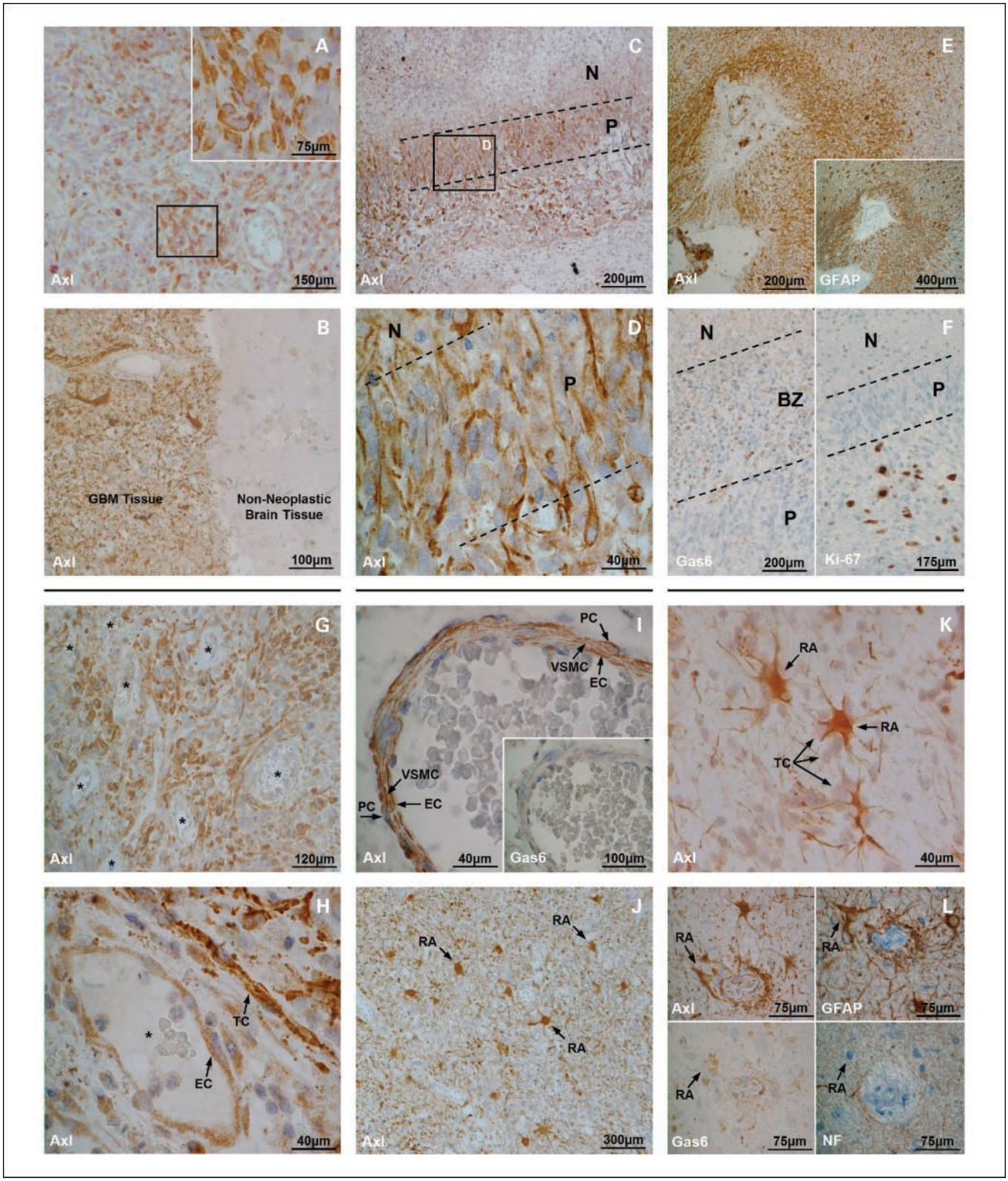

Fig. 2. Immunohistochemical staining pattern of Axl and Gas6 in tumor (GBM), vascular cells, and reactive astrocytes. *A,* Axl expression of GBM cells. *B,* neoplastic (GBM) and nonneoplastic tissue in direct proximity (as an artifact of tissue preparation) show that Axl is only detectable in GBM tissue. *C* to *E,* Axl expression of pseudopalisading tumor cells (*P*), which surround a central necrotic (hypoxic) area (*N*). Axl and GFAP are coexpressed in tumor cells. *F* (*left*), Gas6 expression in the hypoxic border zone (*BZ*) of a necrotic area, but not in pseudopalisades. (*F, right*) adjacent (not migrating) GBM cells show a substantial Ki-67 proliferation rate, whereas pseudopalisading (migrating) tumor cells reveal no cell proliferation (*G* and *H*). Microvascular hyperplasia (*) shows a strong Axl expression of endothelial cells (*EC*) and is surrounded by Axl-positive tumor cells (*TC*). *I*, tumor vessels reveal a strong Axl expression of endothelial cells, vascular smooth muscle cells (*VSMC*), and pericytes (*PC*). *J* and *K,* in the peripheral infiltrative zone of a GBM, Axl and GFAP are coexpressed in reactive astrocytes (*RA*). *L,* reactive astrocytes bordering to the infiltrating boarder zone are Axl and GFAP positive and their astrocytic end feet are in close contact with capillaries.

compared with those with low Axl expression and shows a significant relative increase in the risk for early tumor relapse (P = 0.001; Table 3). Evaluation of Axl/Gas6 coexpression appeared that, in patients with low coexpression levels (n = 25), the median TTP was 7.9 months (range, 1.6-17.0) compared with 3.9 months (range, 2.0-9.1) in those with high levels (n = 10; P = 0.0015 by the log-rank test, Fig. 3B). The adjusted hazard ratio for TTP in the group of high Axl/Gas6 coexpression was 3.6 (95% confidence interval, 1.5-8.4) compared with the group of low expression levels and again showed a significant relative increase in the risk of early tumor relapse (P = 0.003; Table 3). In addition, multivariate binary logistic regression analysis revealed that high Axl expression (P < 0.001) and high Axl/Gas6 coexpression (P = 0.001) were significantly associated with a PFS <6 months (Table 4).

The median OS was 13.1 months (range, 0.8-27.5) in patients with low (n = 31) and 9.4 months (range, 2.4-22.3) in patients with high Axl expression (n = 18; P = 0.057 by the log-rank test, Fig. 3B; P = 0.09 by multivariate Cox regression model, Table 3). In patients with low Axl/Gas6 coexpression (n = 39), the median OS was 13.2 months (range, 0.8-27.5) and 9.2 months in those with high levels (range, 3.3-21.2; n = 9; P = 0.115 by the log-rank test; P = 0.142 by multivariate Cox regression model; Table 3). However, 92% (n = 23) of GBM patients with OS >12 months had a low Axl/Gas6 coexpression compared with only 67% (n = 18) of those with OS <12 months (P = 0.045 by multivariate binary logistic regression analysis; Table 4).

Discussion

Due to the dismal prognosis of GBM with currently available therapies, there is an urgent need for new treatments based on a better understanding of the pathophysiologic and molecular properties of gliomas. The present study shows that the receptor tyrosine kinase Axl and its ligand Gas6 are biologically relevant not only to glioma cells *in vitro* and animal models *in vivo* (10) but also for human gliomas. We show that in human glioma tissue Axl and Gas6 are frequently expressed at the mRNA and protein level, and in GBM patients, high Axl expression and Axl/Gas6 coexpression are significantly associated with shorter TTP and PFS <6 months. In addition, Axl and Axl/Gas6 are related to poorer OS and Axl/Gas6 coexpression is significantly associated with OS <12 months. However, in evaluation of the prognostic significance of Axl and Gas6 expression, TTP and PFS6 are the more reliable study end points compared with OS and OS12 because newly diagnosed GBMs are treated according to a standard therapy protocol until tumor progression, whereas various subsequent therapies are used after tumor progression (13).

Recently, Vajkoczy et al. (10) have shown that inhibition of Axl signaling almost completely suppresses glioma cell migration into a fetal rat brain spheroid and into brain tissue of a mouse i.c. xenograft model. In our study, we show that Axl is predominantly expressed in pseudopalisading glioma cells, characterized by an accumulation of tumor cells around necrotic areas. Such cell formations are composed by a wave of actively migrating tumor cells moving away from a central hypoxic/necrotic area, resulting from an increased metabolic demand and/or intravascular thrombosis (14, 15). In pseudopalisading glioma cells, the subcellular distribution of Axl

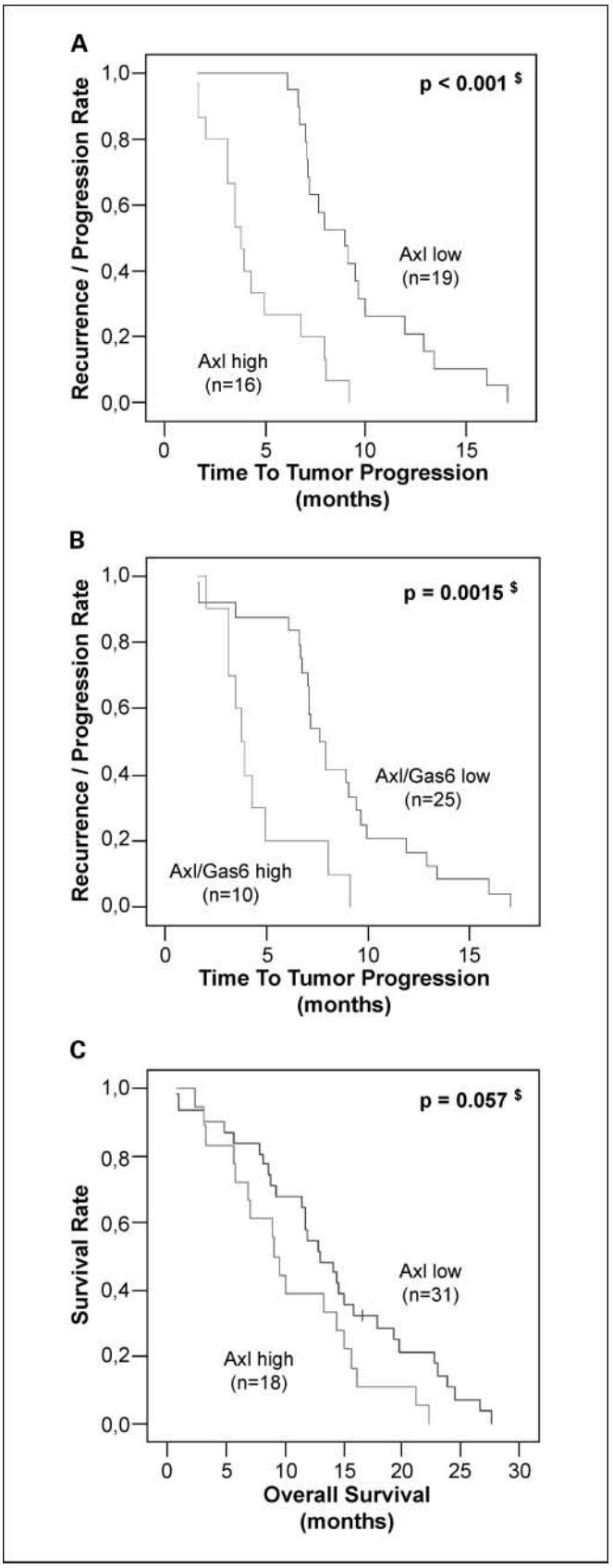

Fig. 3. Prognostic value of Axl and Gas6 expression in GBM patients. *A* to *C*, Kaplan-Meier curves of Axl expression and Axl/Gas6 coexpression in GBM patients related to TTP and OS. $, log-rank test.

Table 4. Association of Axl and Gas6 protein expression to PFS6 and OS12

	Axl			Gas6			Axl/Gas6		
	Low*	High*	*P* †	Low	High	*P* †	Low	High	*P* †
PFS6									
≤6	3 (21)	11 (79)	<0.001	4 (29)	10 (71)	0.055	6 (43)	8 (57)	0.001
>6	29 (76)	49 (24)		22 (58)	16 (42)		35 (92)	3 (8)	
OS12									
≤12	14 (52)	13 (48)	0.145	11 (40)	16 (59)	0.390	18 (67)	9 (33)	0.045
>12	18 (72)	7 (28)		15 (60)	10 (40)		23 (92)	2 (8)	

*Number of cases (percentage), quantification of protein expression: low = GIS ≤ 6 and high = GIS > 6.
† *P* values were calculated by multivariable binary logistic regression analysis, including age (≥60 versus <60 y), KPS (≥80 versus <80%), tumor location (frontal versus nonfrontal), extend of resection (total/subtotal versus partial), chemotherapy (+ versus -), and radiation (+ versus -) as covariables.

expression shows a membrane-accentuated staining pattern, particularly of opposing tumor cells. Due to the cell adhesion properties of the Axl extracellular domain, homophilic Axl-Axl interactions (9, 16) between tumor cells and heterophilic Axl-extracellular matrix binding (17, 18) seem to be important for Axl-mediated glioma cell migration. We also observed an accumulation of Axl-positive tumor cells adjacent to microvascular neoformations. This finding corresponds to a characteristic feature of glioma invasiveness (i.e., invading glial tumor cells spreading along perivascular regions; refs. 19, 20). GFAP, an astrocyte-specific intermediate filament controlling cell shape and cell movement (21, 22), is commonly detectable in glioma cells (23). Our comparative immunohistochemical studies showed that Axl and GFAP are coexpressed in glioma cells of pseudopalisades. This observation suggests a functional association of Axl and GFAP during glioma cell migration. Invading glioma cells are the most difficult to treat and represent the source for local tumor recurrences. Thus, the significantly shorter TTP of GBM patients with high Axl expression may reflect the biological contribution of Axl to a more invasive glioma phenotype.

TTP was also significantly reduced in GBM patients with high Axl/Gas6 coexpression. Such a coexpression was particularly found in nonpseudopalisading tumor cells. As previously shown for other receptor tyrosine kinases (24), Axl and Gas6 may also form autocrine and paracrine stimulation loops. Gas6, originally identified to be induced under growth arrest conditions (7, 8), protects various neuroepithelial cell types from apoptosis *in vitro* (25–27). Cell death due to apoptosis and coagulative necrosis is fundamental in GBM (14, 15). Therefore, we suggest a second biological role of the Axl/Gas6 signaling pathway in glioma cell survival. Whereas Axl was only detectable in gliomas, Gas6 showed a strong expression in neurons of nontumoral tissue. A comparable neuronal expression of Gas6 mRNA has already been reported in the adult rat brain (26) and in primary cultures of rat hippocampal neurons (28, 29). *In vitro* Gas6/Axl signaling attenuated neuronal cell death caused by serum starvation (26), secretory phospholipase A2 (28), and amyloid β protein (29).

Furthermore, Axl and Gas6 were frequently coexpressed in vascular cells of tumor vessels. This included endothelial cells of microvascular hyperplasia, a form of tumor neoangiogenesis related to and induced by hypoxic pseudopalisading cells (14), but also endothelial cells, vascular smooth muscle cells, and pericytes of arterioles and venules adjacent to the GBM tissue. In contrast, such an expression pattern was not observed in vessels of nonneoplastic brain distant to the tumor and nontumoral tissue derived from epilepsy surgery, respectively. In previous *in vitro* and experimental *in vivo* studies, both proteins were found to be expressed in several vascular cell types regulating cell survival, proliferation, and migration (30–36). Axl has also been identified as a key modulator of tube and neointima formation (36) and vascular remodeling (37). In this study, we describe that Axl and Gas6 are also coexpressed in several vascular cell types of tumor vessels in humans *in vivo*, suggesting that Axl and Gas6 may be critically involved in neovascularization of GBMs.

Finally, we observed a strong Axl/GFAP coexpression in reactive astrocytes within and adjacent to the tumor. Reactive astrocytes have crucial functions in modulating the pathology and regenerative response to various brain lesions (38) and are able to secrete a range of astrocytic factors that may protect neuronal integrity and reduce microglial activation (38). In addition, astrocytic end feet, which are in close proximity to the microvessel wall to modulate the blood-brain barrier function (39), show a pronounced Axl staining. In many glial tumors, astroglial-endothelial signaling breaks down and leads to a leakage of capillaries (40) followed by tumor edema. Anti-angiogenic therapy targeting receptor tyrosine kinases, such as vascular endothelial growth factor and platelet-derived growth factor receptors, has the potential to reduce tumor angiogenesis as well as capillary leakage of structurally and functionally abnormal tumor vessels (41). Therefore, we suggest that Axl may also have comparable functions in modulating tumor angiogenesis and blood-brain barrier similar to vascular endothelial growth factor and platelet-derived growth factor receptors.

The aggressiveness of GBM is reflected by a diffuse local infiltration into the brain parenchyma and a high vascularization supporting peripheral tumor growth (15). The present study shows that in glial tumors Axl is frequently expressed in both glioma and vascular cells and its biological effect is represented by the association with poor clinical outcome. At present, targeted therapies inhibiting receptor tyrosine kinases critically involved in oncogenesis and tumor angiogenesis seem to be one of the most promising therapeutic approaches for a variety of neoplastic diseases, including malignant gliomas (42). Therefore, the Axl/Gas6 signaling pathway represents a

novel target for glioma treatment directed against tumor cell migration and survival as well as tumor neoangiogenesis. This could become clinically applicable by designing either small molecular inhibitors or gene expression interference approaches (42).

Acknowledgments

We thank Monika Hainzer, Sarah Rainer, and Marc Sohm (Neurological Research Laboratory); Theresa Kindl and Elisabeth Huber (Clinical Department of Neurology); Robert Moser and Inge Jehart (Institute of Pathology); and Dr. Juergen Schiefermueller for their helpful suggestions and technical support.

References

1. Kleihues P, Sobin LH. World Health Organization classification of tumors. Cancer 2000;88:2887.
2. DeAngelis LM. Brain tumors. N Engl J Med 2001;344:114–23.
3. Stupp R, Mason WP, van den Bent MJ, et al. Radiotherapy plus concomitant and adjuvant temozolomide for glioblastoma. N Engl J Med 2005;352:987–96.
4. Janssen JW, Schulz AS, Steenvoorden AC, et al. A novel putative tyrosine kinase receptor with oncogenic potential. Oncogene 1991;6:2113–20.
5. O'Bryan JP, Frye RA, Cogswell PC, et al. axl, a transforming gene isolated from primary human myeloid leukemia cells, encodes a novel receptor tyrosine kinase. Mol Cell Biol 1991;11:5016–31.
6. Stoeckli ET, Landmesser LT. Axonin-1, Nr-CAM, and Ng-CAM play different roles in the *in vivo* guidance of chick commissural neurons. Neuron 1995;14:1165–79.
7. Manfioletti G, Brancolini C, Avanzi G, Schneider C. The protein encoded by a growth arrest-specific gene (gas6) is a new member of the vitamin K-dependent proteins related to protein S, a negative coregulator in the blood coagulation cascade. Mol Cell Biol 1993;13:4976–85.
8. Varnum BC, Young C, Elliott G, et al. Axl receptor tyrosine kinase stimulated by the vitamin K-dependent protein encoded by growth-arrest-specific gene 6. Nature 1995;373:623–6.
9. Hafizi S, Dahlback B. Signalling and functional diversity within the Axl subfamily of receptor tyrosine kinases. Cytokine Growth Factor Rev 2006;17:295–304.
10. Vajkoczy P, Knyazev P, Kunkel A, et al. Dominant-negative inhibition of the Axl receptor tyrosine kinase suppresses brain tumor cell growth and invasion and prolongs survival. Proc Natl Acad Sci U S A 2006;103:5799–804.
11. Chomczynski P, Sacchi N. Single-step method of RNA isolation by acid guanidinium thiocyanate-phenol-chloroform extraction. Anal Biochem 1987;162:156–9.
12. Remmele W, Schicketanz KH. Immunohistochemical determination of estrogen and progesterone receptor content in human breast cancer. Computer-assisted image analysis (QIC score) versus subjective grading (IRS). Pathol Res Pract 1993;189:862–6.
13. Ballman KV, Buckner JC, Brown PD, et al. The relationship between six-month progression-free survival and 12-month overall survival end points for phase II trials in patients with glioblastoma multiforme. Neuro-oncol 2007;9:29–38.
14. Brat DJ, Castellano-Sanchez AA, Hunter SB, et al. Pseudopalisades in glioblastoma are hypoxic, express extracellular matrix proteases, and are formed by an actively migrating cell population. Cancer Res 2004;64:920–7.
15. Brat DJ, Van Meir EG. Vaso-occlusive and prothrombotic mechanisms associated with tumor hypoxia, necrosis, and accelerated growth in glioblastoma. Lab Invest 2004;84:397–405.
16. Budagian V, Bulanova E, Orinska Z, et al. Soluble Axl is generated by ADAM10-dependent cleavage and associates with Gas6 in mouse serum. Mol Cell Biol 2005;25:9324–39.
17. Bellosta P, Costa M, Lin DA, Basilico C. The receptor tyrosine kinase ARK mediates cell aggregation by homophilic binding. Mol Cell Biol 1995;15:614–25.
18. McCloskey P, Fridell YW, Attar E, et al. GAS6 mediates adhesion of cells expressing the receptor tyrosine kinase Axl. J Biol Chem 1997;272:23285–91.
19. Berens ME, Rief MD, Shapiro JR, et al. Proliferation and motility responses of primary and recurrent gliomas related to changes in epidermal growth factor receptor expression. J Neurooncol 1996;27:11–22.
20. Gladson CL. Expression of integrin $\alpha v\beta 3$ in small blood vessels of glioblastoma tumors. J Neuropathol Exp Neurol 1996;55:1143–9.
21. Mason CA, Edmondson JC, Hatten ME. The extending astroglial process: development of glial cell shape, the growing tip, and interactions with neurons. J Neurosci 1988;8:3124–34.
22. Chintala SK, Kyritsis AP, Mohan PM, et al. Altered actin cytoskeleton and inhibition of matrix metalloproteinase expression by vanadate and phenylarsine oxide, inhibitors of phosphotyrosine phosphatases: modulation of migration and invasion of human malignant glioma cells. Mol Carcinog 1999;26:274–85.
23. Takeuchi H, Sato K, Ido K, Kubota T. Mitotic activity of multinucleated giant cells with glial fibrillary acidic protein immunoreactivity in glioblastomas: an immunohistochemical double labeling study. J Neurooncol 2006;78:15–8.
24. Newton HB. Molecular neuro-oncology and development of targeted therapeutic strategies for brain tumors. Part 1. Growth factor and Ras signaling pathways. Expert Rev Anticancer Ther 2003;3:595–614.
25. Allen MP, Zeng C, Schneider K, et al. Growth arrest-specific gene 6 (Gas6)/adhesion related kinase (Ark) signaling promotes gonadotropin-releasing hormone neuronal survival via extracellular signal-regulated kinase (ERK) and Akt. Mol Endocrinol 1999;13:191–201.
26. Funakoshi H, Yonemasu T, Nakano T, Matumoto K, Nakamura T. Identification of Gas6, a putative ligand for Sky and Axl receptor tyrosine kinases, as a novel neurotrophic factor for hippocampal neurons. J Neurosci Res 2002;68:150–60.
27. Shankar SL, O'Guin K, Kim M, et al. Gas6/Axl signaling activates the phosphatidylinositol 3-kinase/Akt1 survival pathway to protect oligodendrocytes from tumor necrosis factor α-induced apoptosis. J Neurosci 2006;26:5638–48.
28. Yagami T, Ueda K, Asakura K, et al. Effect of Gas6 on secretory phospholipase A(2)-IIA-induced apoptosis in cortical neurons. Brain Res 2003;985:142–9.
29. Yagami T, Ueda K, Asakura K, et al. Gas6 rescues cortical neurons from amyloid β protein-induced apoptosis. Neuropharmacology 2002;43:1289–96.
30. Melaragno MG, Wuthrich DA, Poppa V, et al. Increased expression of Axl tyrosine kinase after vascular injury and regulation by G protein-coupled receptor agonists in rats. Circ Res 1998;83:697–704.
31. Fridell YW, Villa J, Jr., Attar EC, Liu ET. GAS6 induces Axl-mediated chemotaxis of vascular smooth muscle cells. J Biol Chem 1998;273:7123–6.
32. O'Donnell K, Harkes IC, Dougherty L, Wicks IP. Expression of receptor tyrosine kinase Axl and its ligand Gas6 in rheumatoid arthritis: evidence for a novel endothelial cell survival pathway. Am J Pathol 1999;154:1171–80.
33. D'Arcangelo D, Gaetano C, Capogrossi MC. Acidification prevents endothelial cell apoptosis by Axl activation. Circ Res 2002;91:e4–12.
34. Melaragno MG, Cavet ME, Yan C, et al. Gas6 inhibits apoptosis in vascular smooth muscle: role of Axl kinase and Akt. J Mol Cell Cardiol 2004;37:881–7.
35. Collett G, Wood A, Alexander MY, et al. Receptor tyrosine kinase Axl modulates the osteogenic differentiation of pericytes. Circ Res 2003;92:1123–9.
36. Holland SJ, Powell MJ, Franci C, et al. Multiple roles for the receptor tyrosine kinase axl in tumor formation. Cancer Res 2005;65:9294–303.
37. Korshunov VA, Mohan AM, Georger MA, Berk BC. Axl, a receptor tyrosine kinase, mediates flow-induced vascular remodeling. Circ Res 2006;98:1446–52.
38. Hailer NP, Wirjatijasa F, Roser N, et al. Astrocytic factors protect neuronal integrity and reduce microglial activation in an *in vitro* model of *N*-methyl-D-aspartate-induced excitotoxic injury in organotypic hippocampal slice cultures. Eur J Neurosci 2001;14:315–26.
39. Seguin R, Biernacki K, Rotondo RL, Prat A, Antel JP. Regulation and functional effects of monocyte migration across human brain-derived endothelial cells. J Neuropathol Exp Neurol 2003;62:412–9.
40. Abbott NJ, Ronnback L, Hansson E. Astrocyte-endothelial interactions at the blood-brain barrier. Nat Rev Neurosci 2006;7:41–53.
41. Batchelor TT, Sorensen AG, di Tomaso E, et al. AZD2171, a pan-VEGF receptor tyrosine kinase inhibitor, normalizes tumor vasculature and alleviates edema in glioblastoma patients. Cancer Cell 2007;11:83–95.
42. Hutterer M, Gunsilius E, Stockhammer G. Molecular therapies for malignant glioma. Wien Med Wochenschr 2006;156:351–63.